Spatiotemporal dynamics in understanding hand—object interactions

Pietro Avanzini[a], Maddalena Fabbri-Destro[b], Cristina Campi[a], Annalisa Pascarella[c], Guido Barchiesi[d], Luigi Cattaneo[d], and Giacomo Rizzolatti[a,b,1]

[a]Dipartimento di Neuroscienze, Sezione di Fisiologia, Università di Parma, I-43100 Parma, Italy; [b]Brain Center for Motor and Social Cognition, Italian Institute of Technology, I-43100 Parma, Italy; [c]Istituto per le Applicazioni del Calcolo "M. Picone"–Consiglio Nazionale delle Ricerche, I-00185 Rome, Italy; and [d]Center for Mind/Brain Sciences, University of Trento, I-38123 Trento, Italy

This contribution is part of the special series of Inaugural Articles by members of the National Academy of Sciences elected in 2012.

Contributed by Giacomo Rizzolatti, July 31, 2013 (sent for review June 1, 2013)

It is generally accepted that visual perception results from the activation of a feed-forward hierarchy of areas, leading to increasingly complex representations. Here we present evidence for a fundamental role of backward projections to the occipito-temporal region for understanding conceptual object properties. The evidence is based on two studies. In the first study, using high-density EEG, we showed that during the observation of how objects are used there is an early activation of occipital and temporal areas, subsequently reaching the pole of the temporal lobe, and a late reactivation of the visual areas. In the second study, using transcranial magnetic stimulation over the occipital lobe, we showed a clear impairment in the accuracy of recognition of how objects are used during both early activation and, most importantly, late occipital reactivation. These findings represent strong neurophysiological evidence that a top-down mechanism is fundamental for understanding conceptual object properties, and suggest that a similar mechanism might be also present for other higher-order cognitive functions.

object use understanding | top-down effect | conceptual knowledge

Classic studies on the neural basis of visual perception showed that neurons located in progressively higher cortical visual areas in the macaque monkey show increasingly complex properties (1–5). On the basis of these findings, it was proposed that neural substrate crucial for visual perception is represented by the higher-order visual areas of the inferior temporal lobe (6–8). Functional MRI (fMRI) data obtained in humans confirmed these findings (9, 10). These data also suggested that the temporal lobe poles are an even higher integration center, where conceptual object properties (e.g., how an object is commonly used) are represented (11–13).

Visual information processing has been classically considered to be a feed-forward processing, with perception occurring when the areas at the top of the network become active (6, 14–16). On the other hand, rich anatomical evidence shows that there are massive feedback connections going from higher-order areas back to lower-order areas of the visual ventral stream (17–21). Physiological data also provide evidence for cross-talk between visual areas located at different hierarchical level. In fact transcranial magnetic stimulation (TMS) studies (22–26) reported that single-pulse TMS applied over primary visual areas produces significant perceptual impairment in two distinct time windows: an early one and a late one, relative to the presentation of a visual stimulus. The perception impairment caused by stimulation during the second (late) time window was interpreted as a consequence of an interference with a top-down reactivation of V1 (27, 28). A TMS study by Pascual-Leone and Walsh (29) demonstrated that stimulation of area MT/V5 applied 30 ms before the stimulation of V1 affects the activity of this latter region, making participants perceive still rather than moving phosphenes. An analogous cross-talking effect between V5/MT and V1 was reported by Silvanto et al. (30), who administered TMS to these areas during performance of a simple motion-detection task at various time intervals following stimulus offset.

More recently, Camprodon et al. (26) tested the accuracy of healthy volunteers in a visual recognition task. Images of animals (birds or mammals) were briefly presented and subjects were asked to indicate the animal category. Single TMS pulses were applied over the occipital lobe at different latencies relative to the image onset. Visual recognition was impaired when TMS was applied both at 100 and 220 ms. Authors interpreted the perception impairment during the later stimulation as being caused by disruption of a feedback projection to V1 from higher-order areas.

The aim of the present study was to describe the spatiotemporal dynamics underlying the understanding of object use and to assess the possible role of top-down mechanisms in this function. High-density EEG recordings and single-pulse TMS applied to the occipital lobe were used. The EEG experiment consisted of three conditions: (*i*) observation of a static image of a hand grasping an object; (*ii*) observation of a static image of an object followed by a hand grasping it, so as to give the impression of an apparent motion; and (*iii*) observation of a static image of an object followed by a delayed presentation of the hand grasping it.

The cortical activity recorded during all three experimental conditions showed a common pattern characterized by initial activation of occipito-temporal cortical areas followed by a subsequent involvement of higher-order cognitive areas. During this phase, visual area activation was not evident. Subsequently, a strong reactivation of occipito-temporal areas occurred.

To assess whether the late occipito-temporal reactivation plays a role in comprehension of how an object is commonly used, single-pulse TMS was applied during the observation of a static image of a hand grasping an object, over the occipital lobe. Five different latencies with respect to the onset of the grasping-hand image were used. The results showed that TMS significantly disrupted the participants' accuracy not only during the early visual activation, but also during the late reactivation. No significant impairment was found when TMS was delivered during the time window showing higher-order cortical area activation.

Significance

Combining EEG and transcranial magnetic stimulation techniques, we show that reactivation of visual areas plays a fundamental role for understanding conceptual object properties. We suggest that a similar top-down mechanism might also play a role in other higher-order cognitive functions. These results shed a new light on the basic mechanisms underlying perception.

Author contributions: P.A., M.F.-D., C.C., A.P., G.B., L.C., and G.R. designed research; P.A., M.F.-D., C.C., A.P., G.B., and L.C. performed research; P.A., M.F.-D., C.C., A.P., G.B., and L.C. analyzed data; and P.A., M.F.-D., L.C., and G.R. wrote the paper.

The authors declare no conflict of interest.

Freely available online through the PNAS open access option.

[1]To whom correspondence should be addressed. E-mail: giacomo.rizzolatti@unipr.it.

The data strongly support the importance of top-down reactivation for the comprehension of conceptual object properties.

Results

EEG Experiment. A continuous high-density EEG was recorded while participants (n = 10) observed static images of objects grasped by a hand in two different ways: that is, as if to use it or to move it. The task consisted in deciding whether the grip was compatible with the object common use or not. As shown in Fig. 1, three different conditions were used: static hand–object interaction (SI), apparent motion (AM), and gap presentation (GAP). In SI, no other stimulus preceded the grasping image but the fixation cross. In AM, the same stand-alone object was presented for the 500 ms before the image showing the hand–object interaction. There was no gap between the images, so that an apparent motion was perceived. In the GAP condition, the same images of the AM condition were shown, but with a 500-ms gap between the two so as not to elicit the apparent motion perception.

For each subject, event-related potentials (ERP) were computed for the three conditions, after aligning trials on the grasping image presentation (Fig. 1). Subsequently, three grand-averaged ERPs, one for each condition, were computed. These three traces were then submitted to a space-oriented brain electric field analysis (31), returning the sequence of microstates over time for each condition. Functional microstates are characterized by a template map depicting the scalp topography remaining stable from tens to hundreds of milliseconds, and each of them is sustained by a specific brain network (32). A distributed inverse solution was then calculated for each computed template map with a local autoregressive average (LAURA) model, determining the average source localization.

Fig. 2 shows the sequence of microstates relative to all conditions for the first 500 ms after the onset of the hand–object interaction image. The Krzanowski–Lai criterion identified 13 as the optimal number of microstates, explaining the 94.55% of the dataset variance. The first three microstates, covering approximately the first 200 ms, had the same stable topography across all conditions. Subsequently, three different patterns occurred according to the experimental condition.

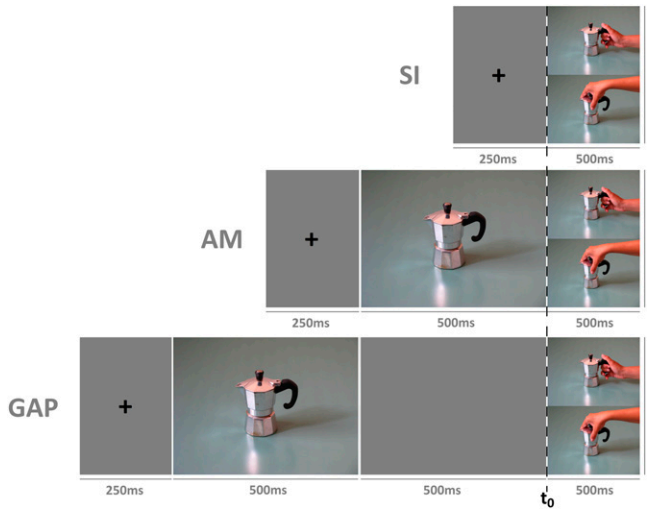

Fig. 1. Experimental design. There were three different conditions: single interaction, apparent motion, and gap presentation. In all conditions, participants were instructed to decide if the hand–object interaction was appropriate for the common use of the object or for moving it. In SI, no other stimulus preceded the grasping image but a fixation cross. In AM, the same stand-alone object was presented for the 500 ms before the image showing the hand–object interaction. No gap was placed between the images, so that an apparent motion was perceived. In the GAP condition, the same two images of the AM condition were interspersed by the presentation of a dark background lasting 500 ms, so as not to elicit the apparent motion perception. Twelve different objects were used. Below each image, the relative duration is reported (milliseconds). The vertical dotted line indicates the timing used for the trial alignment and subsequent ERP computation.

The source localization was computed over each template map obtained by microstate segmentation. Fig. 3 displays brain horizontal sections showing the activated areas for the first three microstates common to all conditions. Microstate 1 was characterized by an activation of the posterior part of inferior temporal lobe. The activation was bilateral, but with a right hemisphere prevalence. The second microstate, starting from about 100 ms following the stimulus onset, showed a strong activation of the occipital areas of the left hemisphere extending into the inferior temporal lobe. Note that this timing (100 ms) corresponds to the arrival of the visual information to the occipital lobe, and is reflected in ERP studies in a positive peak over posterior electrodes (P100). The same positivity is visible in the template map 2 shown in Fig. 2. The last common microstate (M3, lasting from about 150–200 ms) was characterized by an almost complete disappearance of posterior occipito-temporal activity and a very strong activation of the bilateral temporal poles.

Fig. 4 shows the activations corresponding to the microstates in the time window from 200–350 ms. In SI condition, the activation of posterior occipito–temporal areas, which had previously disappeared, reoccurred in the right occipital lobe (yellow microstate in Fig. 4), including the medial visual areas. In contrast, the temporal poles activation, observed at 150–200 ms, was no longer evident. Subsequently, besides a decreasing activation in the temporal lobe, activation of supplementary (SMA) and pre–supplementary motor areas (pre-SMA) occurred (dark green microstate in Fig. 4).

A different pattern was seen in the AM condition. Following the temporal pole activation relative to microstate 3, a clear activation of mesial premotor areas (pre-SMA and SMA) extending laterally into the dorsal premotor cortex was subsequently observed (red microstate in Fig. 4). As in the SI condition, a subsequent reactivation of visual areas occurred (light green microstate in Fig. 4). However, this time the visual reactivation was located in the left hemisphere. As in the SI condition, an activation of SMA/pre-SMA characterized the last microstate.

Finally, the source localization for the GAP condition presented a pattern similar to the SI condition, with a posterior occipito-temporal reactivation following temporal pole activation. Note also that, unlike the AM condition, this reactivation was mainly located in the right hemisphere.

TMS Experiment. As described above, the main result of the EEG study was the reactivation of visual areas following the disappearance of occipital activity in the 150- to 200-ms interval. To assess the significance of this occipital reactivation, we used event-related single-pulse TMS as in an "online virtual lesion paradigm" (33), with the aim of interfering with the neural activity in the occipital regions at different time intervals. The SI condition was tested. Two TMS experiments were carried out in two separate groups of subjects: in the main experiment effective TMS was applied to the occipital lobe and in the control experiment ineffective (sham) TMS was applied. All other experimental conditions (e.g., task, TMS timing) were identical between the two experiments.

Sixteen healthy participants took part in the "effective TMS" experiment. Biphasic single-pulse TMS was delivered to the occipital cortex around the midline over the individual's hotspot for central phosphene induction that had been preliminarily determined. After visual stimulus presentation (duration: 16 ms), single-pulse TMS was applied at five different interstimulus intervals (ISIs: 33, 83, 133, 183, or 217 ms) that were chosen on the basis of the EEG study (see Fig. 2, black marks on the abscissae). Visual stimuli were: (*i*) an object grasped to be used or (*ii*) to be

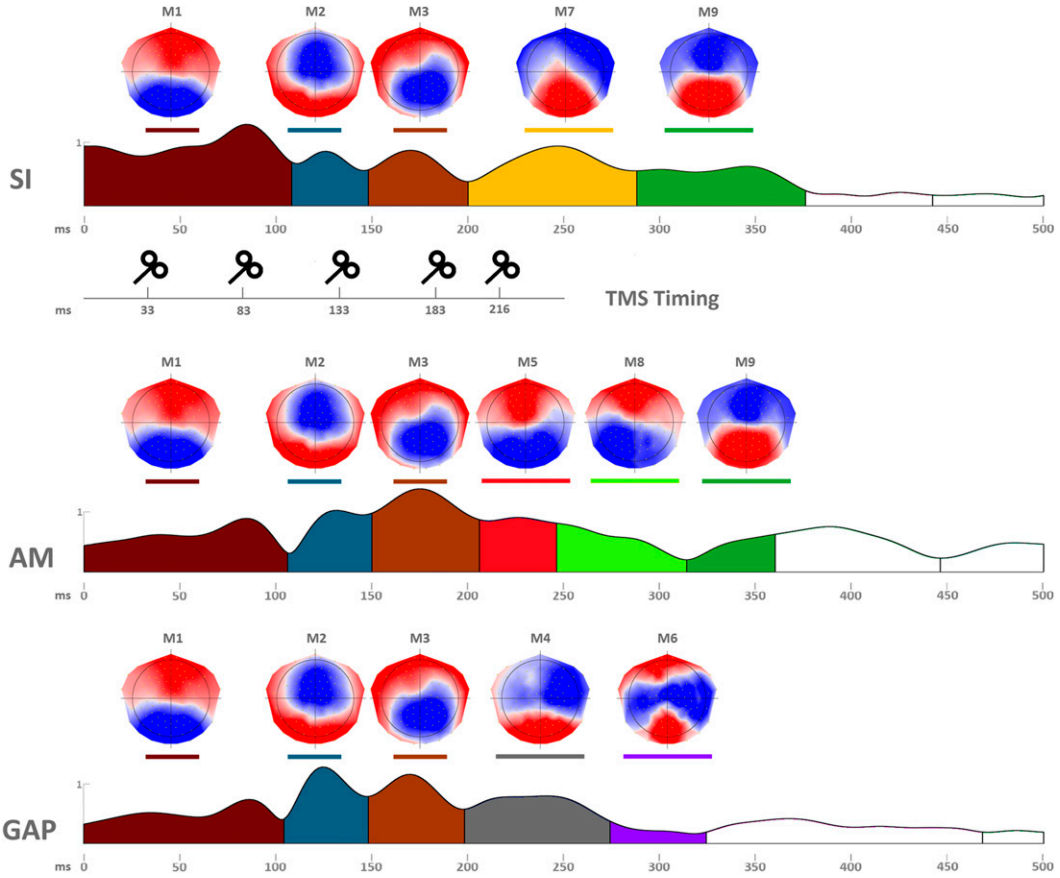

Fig. 2. Microstate segmentation results relative to the three investigated conditions: SI, AM, and GAP. For each condition, microstate sequence (*Lower*) and relative template maps (*Upper*) are presented. Each microstate is indicated by a different color, and their profile reports the GFP, computed for each condition as the variance of the channels over the whole scalp at a given time point. The GFP is always positive and it ranges from 0 up to 1 μV^2. Above each microstate, the relative template map is depicted, underlined with the correspondent color. The *x* axis reports the time (ms) relative to the hand–object interaction appearance. Immediately below the SI condition, the five ISI timings at which TMS was delivered are reported (TMS timing).

moved and (*iii*) the object alone. The task consisted in a forced choice among the three stimulus types.

Eighteen volunteers took part in the "sham TMS" experiment. Accuracy was considered the main psychological variable in both experiments. The data from both experiments were analyzed separately for each of the three stimulus types, with three ANOVAs with the factors TMS (between-subjects, two levels: effective or sham TMS) and ISI (within subjects, five levels: 33, 83, 133, 183, and 217 ms). The results on the "use" stimuli showed a main effect of TMS [$F(1, 32) = 9.61$, $P = 0.004$] and a TMS*ISI interaction [$F(4, 128) = 2.63$, $P = 0.038$], indicating that effective and sham TMS had differential effects on accuracy, according to the ISI at which TMS was applied. In addition, in the "place" stimuli a main effect of TMS [$F(1, 32) = 4.20$, $P = 0.048$] and a TMS*ISI interaction [$F(4, 128) = 3.18$, $P = 0.016$] were found. Finally, the "object" data showed a main effect of TMS [$F(1, 32) = 5.01$, $P = 0.032$] and a trend toward a TMS*ISI interaction [$F(4, 128) = 2.16$, $P = 0.078$]. The accuracy data are indicated in Table 1, together with Bonferroni-corrected planned comparisons between effective and sham-TMS values. The results indicated that effective TMS produced a decrease in accuracy at the 83-ms and 217-ms ISIs for both the "use" and the "place" stimuli, but only at the 83-ms ISI for the "object" stimuli. Fig. 5 illustrates the mean values of accuracy separately for the three video stimulus types.

The response times were analyzed with an ANOVA structured identically to the one used for accuracy values, but no main effects of TMS nor interactions involving the TMS factor were found (minimum $P = 0.14$). Finally, we combined the data of accuracy and response speed in a single inverse efficiency score by dividing the mean response times by the accuracy within each condition (34). This measure accounts for possible results caused by shifts of the criterion or changes in the speed-accuracy trade-off. The ANOVAs performed on the inverse efficiency score confirmed the data on accuracy by showing a TMS*ISI interaction in both the "use" [$F(4, 128) = 5.16$, $P = 0.0007$] and the "place" [$F(4, 128) = 3.39$, $P = 0.01$] conditions. Interestingly, the ANOVA carried out on the "object" condition confirmed the trend observed with accuracy values by showing a significant TMS*ISI interaction [$F(4, 128) = 3.64$, $P = 0.008$].

Discussion

General Findings. In the present study we investigated the spatiotemporal dynamics of the network underlying object conceptual knowledge and, more specifically, how an object is used, by using high-density EEG recordings and single-pulse TMS technique. The EEG data showed that, in all experimental conditions, the first observed activation following stimulus presentation occurred in the inferior temporal lobe (microstate 1). Because this activation preceded the arrival of stimulus information to the cerebral cortex, it is likely that the origin of this activation has to be related to the expectancy of the presentation of object stimuli (cup, scissors, hammer, and so forth) used in the present study. The first stimulus-related activation was observed in microstate 2, where there was a strong activation of the occipito-temporal cortex. Subsequently, the activity moved rostrally toward the temporal pole, bilaterally (microstate 3). During this phase, the occipital activation was no more apparent.

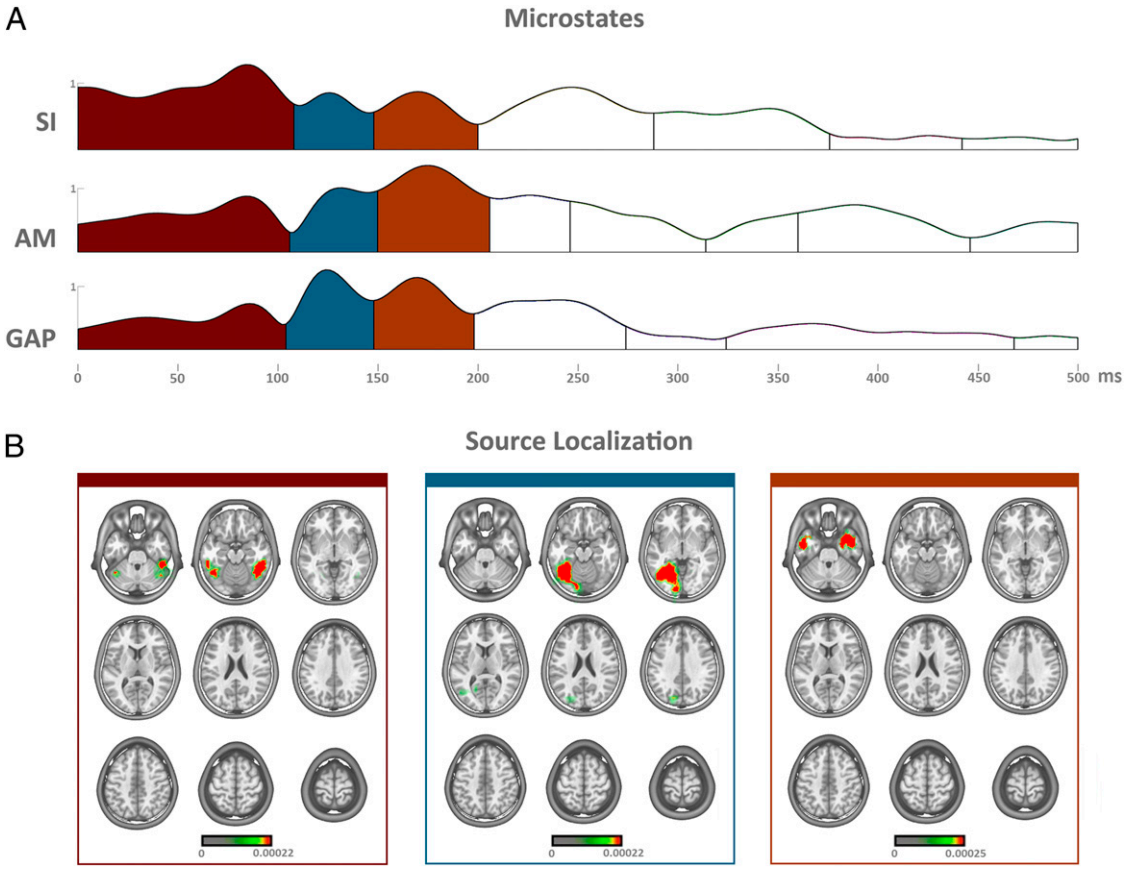

Fig. 3. Analysis of the first part of stimulus processing, common to all conditions. (*A*) The microstate sequence is reported for all conditions relative to the first 200 ms after the hand–object interaction appearance. The microstates not common to all conditions are shown in white. (*B*) For each microstate, the relative source localization is shown on axial slices from a MNI152 brain template. Above each localization, a colored line corresponding to the relative microstate is reported. The color code for the current density in the brain space ranges from 0 to 0.0005 A^2/m^2.

The most interesting result of our study was the demonstration that, following the microstate dominated by activation of higher-order cognitive areas (i.e., microstate 3), a marked reactivation of occipito-temporal visual areas occurred. Most importantly, interference with the occipital lobe activity determined by single-pulse TMS in the time period corresponding to these microstates determined a profound decrease in the participants' accuracy in assessing the object use. This accuracy decrease was also observed during the first visual activation following stimulus presentation (microstate 2). In contrast, the stimulation of the occipital lobe during microstate 3, when temporal lobe poles but not the posterior visual areas were active, was ineffective in changing the behavioral performance, further demonstrating the functional time separation between the two visual activations. Note that although the stimulation at 83 ms disrupted the capacity to discriminate the three stimuli one from another, the "late" stimulation (216 ms) specifically impaired the discrimination of whether the object was grasped to be used or to be moved. This finding suggests that a mere visual degradation is not sufficient to explain the accuracy decrease per se.

There is some disagreement in literature concerning the functional role of temporal poles in conceptual knowledge. In a recent meta-analysis, Binder et al. (35) described an extensive network of regions involved in semantic knowledge, not including, however, the temporal lobe pole. In contrast, clinical studies clearly suggest that this sector of the temporal lobe is crucially involved in conceptual knowledge (11, 12). This view was recently confirmed by an fMRI study of Peelen and Caramazza (13). These authors presented objects that differed on two dimensions and namely (*i*) where the object is typically found and, most importantly for the present study, (*ii*) how the object is commonly used. Results showed that conceptual object representation was localized in the temporal pole, and it was distinct from the localization of object perceptual properties, mostly encoded in the temporal lobe (Brodmann area 37), and of low-level visual features, located in the visual areas of the occipital lobe. These authors argue that the particular anatomical location of the temporal lobe poles in the skull might have determined negative results in fMRI studies.

Our data are in full agreement with the view of Peelen and Caramazza (13) on the anatomical circuit underlying conceptual knowledge. The authors confirm that the occipital areas, the temporal lobe, and the temporal lobe poles are all involved in determining the knowledge of how an object is used. However, given the high time resolution of the EEG technique, our data also showed the timing of the sequential activation of these areas: first, a forward process from the occipito-temporal region to the temporal lobe poles, then a backward process reactivating the temporo-occipital region.

Condition Differences. The cortical activation pattern observed in the three experimental conditions of the present study were not identical. In the SI condition as well as in the GAP condition, the reactivation of the posterior temporo-occipital areas concerned the right hemisphere. In contrast, in the AM condition, following the conceptual coding of the stimulus, there was an additional motor activation that included the mesial and the dorsal premotor areas. This activation was followed, as in the other conditions, by the occipito-temporal reactivation that, unlike in the SI and GAP conditions, was mostly located in the left hemisphere. It is important to note that the premotor activation occurred only in that condition in which virtual motion stimuli

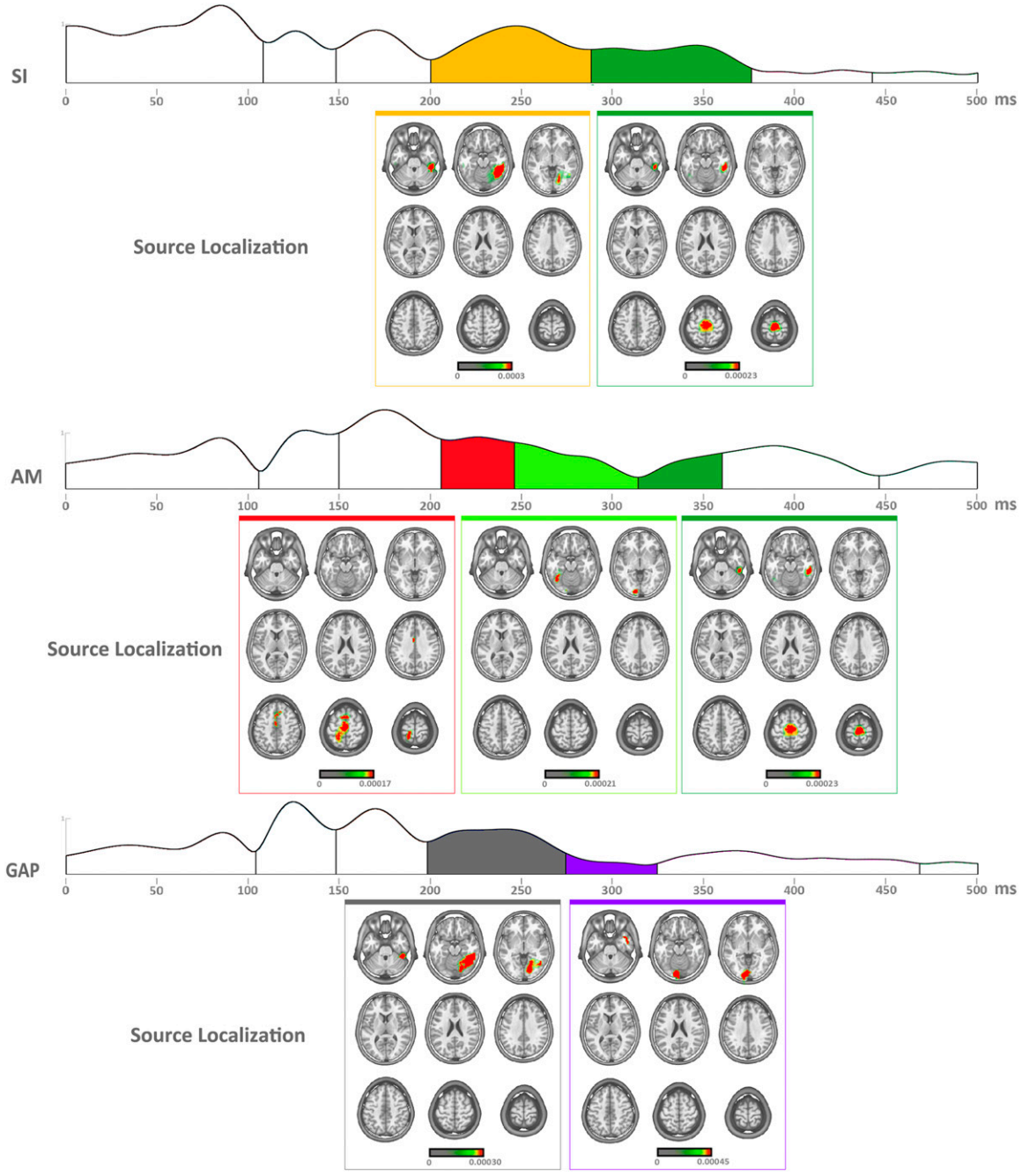

Fig. 4. Microstate analysis and source localization for the processing specific for each condition: SI, AM, and GAP. The microstate sequence is illustrated for the time following the 200 ms after the hand–object interaction appearance. The previous microstates, common to all conditions, are presented in white. For each microstate and condition, the relative source localization is shown on axial slices from a MNI152 brain template. Above each localization a colored line corresponding to the relative microstate is reported. The color code for the current density in the brain space ranges from 0 to 0.0005 A^2/m^2.

were presented. The interpretation of this finding can only be hypothetical. However, it is plausible that the motor activation reflected a kind of automatic "rehearsal" of the virtual movement, possibly to get a complete conceptual understanding of whether the object was indeed correctly used.

Consistent with the notion of an involvement of motor areas for full conceptual understanding in the AM condition is the reactivation, in this condition, of the left occipito-temporal lobe rather than of the right one observed in the other two conditions. The left hemisphere activation fits with the classic notion that this hemisphere is the praxic hemisphere involved in action organization (36–38), as well as in action understanding (39, 40).

Finally, it must be stressed that in the present study we have not presented stimuli representing the dynamic aspects of the object use. The only condition in which some movement could be perceived was the AM condition. Also in this case, however, the movement was only apparent and lacked the dynamic aspects characterizing real movements. It is probably because of these "no-movement" stimuli that no activation of the parieto-frontal circuit, known to mediate the dynamic action understanding, was present. Also in the AM condition, the static aspects of object use dominated and the task was essentially performed by the visual ventral stream and culminated in temporal pole activation.

Table 1. Mean values of accuracy and response times in the effective-TMS (n = 16) and in the sham-TMS (n = 18) groups

	Use			Place			Object		
ISI (ms)	Effective TMS	Sham TMS	*P* value	Effective TMS	Sham TMS	*P* value	Effective TMS	Sham TMS	*P* value
Accuracy									
33	0.59 (0.08)	0.66 (0.07)	0.16	0.7 (0.08)	0.75 (0.09)	0.44	0.89 (0.05)	0.93 (0.03)	0.17
83	**0.5 (0.1)**	**0.69 (0.06)**	**0.002**	**0.65 (0.08)**	**0.78 (0.06)**	**0.008**	**0.84 (0.06)**	**0.93 (0.03)**	**0.008**
133	0.53 (0.08)	0.65 (0.06)	0.02	0.65 (0.09)	0.74 (0.07)	0.08	0.83 (0.06)	0.93 (0.04)	0.02
183	0.59 (0.08)	0.66 (0.05)	0.09	0.69 (0.09)	0.73 (0.08)	0.40	0.9 (0.06)	0.92 (0.04)	0.56
217	**0.48 (0.09)**	**0.69 (0.06)**	**0.0005**	**0.6 (0.09)**	**0.76 (0.08)**	**0.007**	0.91 (0.05)	0.92 (0.04)	0.55
Response time									
33	889 (59)	952 (81)	0.25	914 (62)	955 (84)	0.43	720 (79)	759 (36)	0.38
83	914 (84)	983 (100)	0.29	901 (68)	960 (88)	0.28	738 (90)	757 (33)	0.69
133	934 (78)	994 (89)	0.33	936 (77)	957 (80)	0.70	739 (78)	746 (35)	0.87
183	959 (80)	980 (98)	0.74	919 (64)	970 (84)	0.32	714 (79)	768 (41)	0.24
217	959 (67)	974 (82)	0.79	927 (76)	959 (78)	0.55	739 (78)	789 (48)	0.30

The 95% confidence intervals are provided in parenthesis. Decreased performance is indicated by lower values of accuracy but by higher values of response times. The rightmost column in each section indicates the *P* value resulting from the planned *t* tests comparing the accuracy of the two groups at each ISI. Given that for this interaction the planned comparisons were repeated five times, the significance threshold was corrected to $P = 0.01$ and, accordingly, significant values are presented in bold.

Theoretical Considerations. As already discussed in the introductory paragraphs, the classic view of visual perception is a feed-forward process starting from primary visual cortex and terminating with the activation of higher-order cognitive areas. However, an alternative hypothesis was proposed by Hochstein and Ahissar (41; but see also ref. 42). According to this hypothesis, the "processing along the feedforward hierarchy of areas, leading to increasingly complex representations, is automatic and implicit, while conscious perception begins at the hierarchy's top, gradually returning downwards as needed" (41). Our findings showed a similar mechanism for understanding how an object is used.

However, before discussing the physiological mechanisms underlying the top-down effect, it is important to stress, as mentioned above, that how an object is used—in our experiment—was inferred from static and not moving stimuli, with the possible exception of the AM condition, in which the perception was helped by apparent motion. Given this constraint, it is not surprising that in our experiment the top-down effect was flowing from higher-order cognitive areas like the temporal poles, rather than from the motor centers of action observation/action execution network. In these static conditions, the temporal poles appeared to play the major role in object's use understanding, with the reactivation of occipital areas providing the details necessary for full perception.

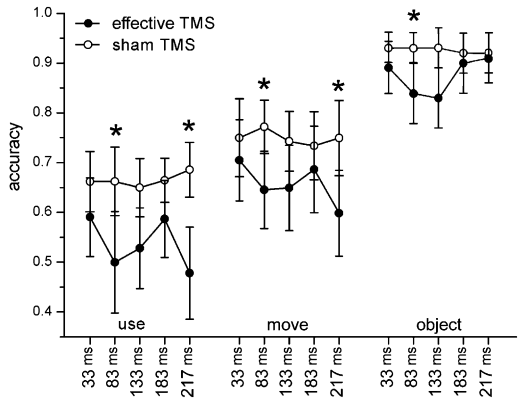

Fig. 5. TMS results. The figure shows the average response accuracy for the three stimulus types (use, move, and object) at different TMS times after the stimulus onset (33, 83, 133, 183, and 217 ms). Black circles indicate "effective" TMS and white circles indicate "sham" TMS. Asterisks indicate the statistical significance within the same ISI between the two stimulations. Error bars indicate 95% confidence intervals.

The top-down model presented herein suggests that understanding how an object is used is required in the activation of the higher-order cognitive areas, with or without the help of the motor system, but with a fundamental reactivation of posterior temporo-occipital areas. The TMS data provide strong support for the necessity of this activation for an accurate understanding of object use.

Another way to account for backward activation in perception is that proposed by a predictive coding framework (43, 44). In this view, each level of cortical hierarchy employs a generative model to predict a representation conveyed by backward connections to the lower level, where it is compared with the representation coming from the subordinate level to produce a prediction error. This prediction error is then sent back to the higher level, via forward connections, to adjust the neuronal representation of sensory cause (44).

A possible weakness of this model is that it requires a prior expectation about the presented object or the goal of the observed action. The number of these expectations, however, could be exceedingly high, rendering its implementation rather difficult. In contrast, when expectations are reduced, this model appears to be well suited for account for the cross-talking between higher-order and lower-order cortical areas.

The preactivation of the inferior temporal lobe observed in the present study could be considered evidence in favor of the predictive framework. Before stimulus occurrence, a representation of the perceptual features of the expected objects is already present. However, the temporal course of the activation of different areas seems to be discrete rather than continuous, as postulated by the predictive framework. One must say here, however, that the technique we used favors the identification of the global activation peak relative to the activity distribution over the whole cortex. Summing up, although the predictive hypothesis is still plausible, we are inclined to favor the reverse hierarchy theory proposed by Hochstein and Ahissar (41) to explain our finding.

In conclusion, we suggest that the reactivation of the posterior temporo-occipital areas is a general mechanism fundamental for understanding conceptual object properties and possibly also valid for other higher-order cognitive functions. In this last case, the top-down effect should start not from the temporal pole but from other key areas endowed with higher-order representations.

Experimental Procedures

EEG Study. ***Participants.*** Ten healthy volunteers (three males and seven females) participated in the EEG experiment. The particpants had normal or corrected-to-normal vision and no history of neurological or psychiatric disorder. The mean age of the volunteers was 27.2 ± 5.2 y old. All were right-handed, as ascertained by the Edinburgh Handedness Inventory (45). The volunteers gave written informed consent for their participation. Ethical approval was obtained from the Ethics Committee of the Medical Faculty at the University of Parma.

Stimuli and procedure. Static stimuli were used so as to accurately identify the precise temporal dynamics (i.e., on a millisecond time scale) underlying how the object is used. Then, the stimuli set comprised static images depicting two possible hand–object interactions: that is, "grasp to use the object" or "grasp to move it." In the first case, the object was grasped according to its common use, whereas in the latter case the grasping was not compatible with the common use. Twelve different objects were used: screwdriver, coffee pot, key, knife, spoon, scissors, fork, hammer, mug, toothbrush, coffee cup, and glass.

As shown in Fig. 1, three different conditions were used: static interaction, apparent motion, and gap presentation. In SI, no other stimulus preceded the grasping image but a fixation cross. In AM, the same standalone object was presented for the 500 ms before the image showing the hand–object interaction. No gap was placed between the images, so that an apparent motion was perceived. In the GAP condition, the same two images of the AM condition were interspersed by the presentation of a dark background lasting 500 ms, so as not to elicit the apparent motion perception. For all three conditions, "use" and "move" trials were balanced.

Each trial (Fig. 1) started presenting a fixation cross (250 ms) to focus the gaze of the participants on the center of the monitor. Subsequently, the sequence of images, the number of which varied according to the presented condition (one for SI, two for AM, three for GAP), was shown. Each static image was presented for 500 ms. Finally, a dark gray background was used for intertrial time (random duration, range 1,000–3,000 ms). A total of 360 trials were administered, 120 for each condition (SI, AM, and GAP, five repetitions for each grasping image), which took up to a total of 30 min recording time, equally subdivided in two blocks. Visual stimuli were presented using E-Prime software (www.pstnet.com). The participants were comfortably seated 70 cm away from a 19-inch monitor where stimuli were presented centrally, subtending a horizontal visual angle smaller than 10°.

Participants were instructed to decide whether the observed hand–object interaction was compatible or not with the common use of the object. Only when a question mark appeared on the screen (500 ms after grasping image offset, 10% of trials, randomly distributed), were they required to state aloud their choice.

EEG recording. Continuous EEG was acquired using the 128-channel Geodesic EEG System (Electrical Geodesics) and the HydroCel Geodesic Sensor Net that arrays the sensors (AgCl-coated electrodes) in a geodesic pattern over the surface of the head. This sensor net included 19 contacts at the equivalent 10–20 system locations. Consistent positioning was achieved by aligning the sensor net with skull landmarks (nasion, vertex, and preauricular points). With high-input impedance amplifiers (Net Amps300), low-noise EEG was obtained with sensor–skin impedances maintained below 100 kΩ. The signal was digitized at 500-Hz sampling rate (0.01 Hz high-pass filter), recorded with a vertex reference.

EEG data analysis. EEG data were analyzed off-line by means of NetStation software (Electrical Geodesics) and homemade MATLAB scripts (The Mathworks). Continuous recordings were segmented in epochs lasting 2,000 ms, each including the 1,000-ms preceding and the 1,000-ms following the grasping-image onset. For artifact detection and removal, each participants' epoch-file was high-pass filtered (1 Hz), imported in BrainVision Analyzer software, and analyzed by means of independent component analysis (46), then back-transformed, excluding components whose topography and time-course endowed eye (blink and saccades), cardiac, and muscular artifacts. A mean number of 13.1 ± 3.1 components were removed. The resulting epoch files were further visually inspected to exclude remaining bad trials (about 6% of trials removed) and rereferenced against the average signal of all electrodes located above the axial plane passing through fronto-polar and occipital electrodes.

Epoch-files were band-pass filtered (1–70 Hz). The outermost belt of electrodes of the sensor net was discarded because they are more prone to show residual muscular artifacts. Eventually, only 110 electrodes entered subsequent analyses. The ERP for each subject and condition was computed.

The first 500 ms after grasping-image onset were used, regardless of the presented stimuli (use or move), to compute three group-averaged ERPs, one for each condition (SI, AM, and GAP). Subsequently, the results were submitted to a space-oriented brain electric field analysis. This method relies on the notion of functional brain microstates introduced in the 1980s by Lehmann et al. (31). The method is based on the observation that the electric brain activity does not vary randomly over time after a stimulus onset but, rather, that some brain topographies remain stable over time from tens to hundreds of milliseconds (32). Each stable brain topography (named microstate) is sustained by a specific brain network and reflects a specific functional brain state (31, 32).

The analysis procedure implemented for identifying the periods of topographic stability within and between experimental conditions is a modified agglomerative hierarchical clustering (47), termed "atomize and agglomerate hierarchical clustering," applied here on the group-averaged ERPs. Cluster analysis is reference-free and insensitive to amplitude modulation of the same scalp potential field across conditions, because normalized maps are compared. The output is a set of template maps (i.e., microstates) describing the group-averaged ERPs. The number of microstates explaining most of the considered dataset variance was determined by a modified Krzanowski–Lai criterion (48).

To statistically assess the validity of the microstate results, we applied a fitting procedure based on the calculation of the spatial correlation between single-subject ERPs and template maps (47, 49). For each subject and condition, the amount of time characterized by each template was obtained in a specific time window of interest. A repeated-measurements ANOVA was subsequently performed with MAP and CONDITION as factors, with the aim to validate at the single subject level the differences highlighted by the microstate segmentation. The microstate and back-fitting analysis, performed across time and experimental conditions, allowed us to determine whether and when different experimental conditions engaged distinct scalp potential configurations, which in turn call for different intracranial generators (47).

Once we had assessed the time windows showing different maps according to conditions, we calculated a distributed inverse solution with the LAURA model. This model is based on reconstruction of the brain electric activity in each point of a 3D grid of solution points. Each solution point is considered as a possible location of a current source, thus there is no a priori assumption on the number of dipoles in the brain. The computation provides a unique configuration of activity at each solution point that explains the surface measurements. Because an infinite number of distributions of current sources within this 3D grid of solution points can lead to exactly the same scalp-potential map, the inverse problem is highly underdetermined. This underdetermined nature of the source model further necessitates the application of different assumptions to identify the "optimal" or "most likely" solution. LAURA attempts to incorporate biophysical laws as constraints driving the calculation of a unique solution. This approach is capable of dealing with multiple simultaneously active sources. The solution space was computed on a locally spherical head model with anatomical constraints (50) and comprised 3,001 solution points equidistantly distributed within the brain structures of the Montreal Neurological Institute (MNI152) average brain. The inverse solution was computed for each template map returned by microstate segmentation, determining for each condition the temporal sequence of cortical activations.

TMS Study. ***Participants.*** The effective TMS experiment was carried out on 16 participants (6 male, 10 female, mean age 27 y) and the sham-TMS experiment was performed on 18 participants (9 male, 9 female, mean age 24 y). The study was conducted in the University of Trento facilities, was approved by the Local Ethical Committee for human studies (protocol 2009–033), and was conducted in compliance with the Helsinki Declaration of 1975, as revised in 1983. All participants were screened for contraindications to TMS (51) and gave written informed consent to participate in the experiment.

Visual stimuli and task. Stimuli were color pictures sized 54 × 40 pixels showing 12 different objects that could be grasped by a hand in order either to be moved (move) or to be used (use) or presented alone (object). The objects were always presented in the center of the screen in two symmetrical orientations (i.e., the affordance of the object could be placed on the left or on the right side of the picture). Each object in each condition and in each orientation was presented five times randomly, for a total of 360 stimuli (12 objects × 3 stimulus types × 2 orientations × 5 times). Visual stimuli were presented on a PC computer using E-Prime software (www.pstnet.com). Screen refresh was set to 60 Hz, and display resolution was set to 1,280 × 768 pixels. The distance of the participant from the screen was 60 cm. The visual angle of the stimuli was therefore of around 1.5°. Participants performed a forced-choice task, in which they had to indicate if the just observed picture showed a standalone object (object) or a hand placed on the object as for moving it (move) or for using it (use). Subjects had to press three

different keyboard keys using their index, middle, and ring fingers. The key-response coding was randomized across participants. Response type and response time were logged for off-line analysis.

TMS. Biphasic TMS pulses were generated by a MagPro 3100 stimulator (MagVenture) and delivered through a 70-mm diameter figure-of-eight coil (model MC-B70; MagVenture). In the effective TMS experiment, the individual phosphene threshold was assessed as the intensity required for the participant to perceive phosphenes in 5 of 10 consecutive trials. Stimulation intensity was then set to 150% of phosphene threshold and corresponded on average to 87% of maximum stimulator output. In the sham-TMS experiment the intensity was systematically set at 90% of maximal stimulator output in all subjects but the coil was positioned 2 cm away from the scalp. TMS pulses in both experiments were delivered at 33-, 83-, 133-, 183-, or 217-ms ISIs from the onset of the visual stimulus.

Procedure. Participants sat comfortably on a chair, laying their head on a chinrest to keep the head still. The magnetic coil was kept steady in position on the participants' scalp or away from it, according to the experiment, thanks to a mechanical arm. At the onset of each trial a black empty circle of the same size of the grasp pictures, was presented in the center of the screen for 1,000 ms on a white background. The circumference was replaced by a stimulus, presented for one frame (16 ms). Afterward another black circumference identical to the previous one was presented, followed by a white screen lasting 1,000 ms. Participants had to respond within 2,000 ms after the presentation of the stimulus. A single TMS pulse at one of the five ISIs was delivered in a pseudorandom order. Communication between the stimulus-presentation computer and the TMS was ensured by means of the parallel port and a 1401 micro Mk-II unit (Cambridge Electronic Design).

ACKNOWLEDGMENTS. We thank M. A. Arbib, J. B. Bonaiuto, M. Giese, and M. Gardner for helpful comments on previous versions of this paper; C. M. Michel for technical supervision; and A. Caramazza for his theoretical suggestions. This study was supported by the Advanced European Research Grant COGSYSTEM (to G.R.), European Union Grant MEG-MRI, and by a fund ("Fondo regionale") for research in Neuroscience from Regione Emilia-Romagna.

1. Hubel DH, Wiesel TN (1968) Receptive fields and functional architecture of monkey striate cortex. *J Physiol* 195(1):215–243.
2. Gross CG, Rocha-Miranda CE, Bender DB (1972) Visual properties of neurons in inferotemporal cortex of the Macaque. *J Neurophysiol* 35(1):96–111.
3. Maunsell JH, Newsome WT (1987) Visual processing in monkey extrastriate cortex. *Annu Rev Neurosci* 10:363–401.
4. Tanaka K (1996) Inferotemporal cortex and object vision. *Annu Rev Neurosci* 19: 109–139.
5. Orban GA (2008) Higher order visual processing in macaque extrastriate cortex. *Physiol Rev* 88(1):59–89.
6. Gross CG, Bender DB, Rocha-Miranda CE (1969) Visual receptive fields of neurons in inferotemporal cortex of the monkey. *Science* 166(3910):1303–1306.
7. Ungerleider LG, Mishkin M (1982) Two cortical visual systems. *Analysis of Visual Behavior*, eds Ingle MA, Goodale MI, Masfield RJW (MIT Press, Cambridge, MA), pp 549–586.
8. Tanaka K (2000) Mechanisms of visual object recognition studied in monkeys. *Spat Vis* 13(2–3):147–163.
9. Orban GA, Van Essen D, Vanduffel W (2004) Comparative mapping of higher visual areas in monkeys and humans. *Trends Cogn Sci* 8(7):315–324.
10. Kanwisher N (2010) Functional specificity in the human brain: A window into the functional architecture of the mind. *Proc Natl Acad Sci USA* 107(25):11163–11170.
11. Damasio H, Grabowski TJ, Tranel D, Hichwa RD, Damasio AR (1996) A neural basis for lexical retrieval. *Nature* 380(6574):499–505.
12. Patterson K, Nestor PJ, Rogers TT (2007) Where do you know what you know? The representation of semantic knowledge in the human brain. *Nat Rev Neurosci* 8(12): 976–987.
13. Peelen MV, Caramazza A (2012) Conceptual object representations in human anterior temporal cortex. *J Neurosci* 32(45):15728–15736.
14. Hubel DH, Wiesel TN (1998) Early exploration of the visual cortex. *Neuron* 20(3): 401–412.
15. Marr D (2010) *Vision: A Computational Investigation into the Human Representation and Processing of Visual Information* (MIT Press, London, UK and Cambridge, MA).
16. Felleman DJ, Van Essen DC (1991) Distributed hierarchical processing in the primate cerebral cortex. *Cereb Cortex* 1(1):1–47.
17. Kennedy H, Bullier J (1985) A double-labeling investigation of the afferent connectivity to cortical areas V1 and V2 of the macaque monkey. *J Neurosci* 5(10):2815–2830.
18. Webster MJ, Ungerleider LG, Bachevalier J (1991) Connections of inferior temporal areas TE and TEO with medial temporal-lobe structures in infant and adult monkeys. *J Neurosci* 11(4):1095–1116.
19. Rockland KS, Van Hoesen GW (1994) Direct temporal-occipital feedback connections to striate cortex (V1) in the macaque monkey. *Cereb Cortex* 4(3):300–313.
20. Logothetis NK, Sheinberg DL (1996) Visual object recognition. *Annu Rev Neurosci* 19: 577–621.
21. Suzuki W, Saleem KS, Tanaka K (2000) Divergent backward projections from the anterior part of the inferotemporal cortex (area TE) in the macaque. *J Comp Neurol* 422(2):206–228.
22. Corthout E, Uttl B, Walsh V, Hallett M, Cowey A (1999) Timing of activity in early visual cortex as revealed by transcranial magnetic stimulation. *Neuroreport* 10(12): 2631–2634.
23. Heinen K, Jolij J, Lamme VAF (2005) Figure-ground segregation requires two distinct periods of activity in V1: A transcranial magnetic stimulation study. *Neuroreport* 16(13):1483–1487.
24. Laycock R, Crewther DP, Fitzgerald PB, Crewther SG (2007) Evidence for fast signals and later processing in human V1/V2 and V5/MT+: A TMS study of motion perception. *J Neurophysiol* 98(3):1253–1262.
25. Kammer T (2007) Visual masking by transcranial magnetic stimulation in the first 80 milliseconds. *Adv Cogn Psychol* 3(1-2):177–179.
26. Camprodon JA, Zohary E, Brodbeck V, Pascual-Leone A (2010) Two phases of V1 activity for visual recognition of natural images. *J Cogn Neurosci* 22(6):1262–1269.
27. Silvanto J, Cowey A, Lavie N, Walsh V (2005) Striate cortex (V1) activity gates awareness of motion. *Nat Neurosci* 8(2):143–144.
28. Koivisto M, Mäntylä T, Silvanto J (2010) The role of early visual cortex (V1/V2) in conscious and unconscious visual perception. *Neuroimage* 51(2):828–834.
29. Pascual-Leone A, Walsh V (2001) Fast backprojections from the motion to the primary visual area necessary for visual awareness. *Science* 292(5516):510–512.
30. Silvanto J, Lavie N, Walsh V (2005) Double dissociation of V1 and V5/MT activity in visual awareness. *Cereb Cortex* 15(11):1736–1741.
31. Lehmann D, Ozaki H, Pal I (1987) EEG alpha map series: Brain micro-states by space-oriented adaptive segmentation. *Electroencephalogr Clin Neurophysiol* 67(3):271–288.
32. Michel CM, Seeck M, Landis T (1999) Spatiotemporal dynamics of human cognition. *News Physiol Sci* 14:206–214.
33. Robertson EM, Théoret H, Pascual-Leone A (2003) Studies in cognition: The problems solved and created by transcranial magnetic stimulation. *J Cogn Neurosci* 15(7): 948–960.
34. Townsend JT, Ashby FG (1983) *The Stochastic Modelling of Elementary Psychological Processes* (Cambridge Univ Press, Cambridge).
35. Binder JR, Desai RH, Graves WW, Conant LL (2009) Where is the semantic system? A critical review and meta-analysis of 120 functional neuroimaging studies. *Cereb Cortex* 19(12):2767–2796.
36. Heilman KM, Rothi LJ, Valenstein E (1982) Two forms of ideomotor apraxia. *Neurology* 32(4):342–346.
37. De Renzi E, Faglioni P (1999) Apraxia. *Handbook of Clinical and Experimental Neuropsychology*, eds Denes G, Pizzamiglio L (Psychology Press, Hove, UK), pp 421–440.
38. Liepmann H (1908) *Drei Aufsätze aus dem Apraxiegebiet* (Karger, Berlin).
39. Rothi LJ, Heilman KM, Watson RT (1985) Pantomime comprehension and ideomotor apraxia. *J Neurol Neurosurg Psychiatry* 48(3):207–210.
40. Pazzaglia M, Pizzamiglio L, Pes E, Aglioti SM (2008) The sound of actions in apraxia. *Curr Biol* 18(22):1766–1772.
41. Hochstein S, Ahissar M (2002) View from the top: Hierarchies and reverse hierarchies in the visual system. *Neuron* 36(5):791–804.
42. Kanwisher N (1991) Repetition blindness and illusory conjunctions: Errors in binding visual types with visual tokens. *J Exp Psychol Hum Percept Perform* 17(2):404–421.
43. Kilner JM, Friston KJ, Frith CD (2007) Predictive coding: An account of the mirror neuron system. *Cogn Process* 8(3):159–166.
44. Friston K (2012) Prediction, perception and agency. *Int J Psychophysiol* 83(2):248–252.
45. Oldfield RC (1971) The assessment and analysis of handedness: The Edinburgh inventory. *Neuropsychologia* 9(1):97–113.
46. Delorme A, Makeig S (2004) EEGLAB: An open source toolbox for analysis of single-trial EEG dynamics including independent component analysis. *J Neurosci Methods* 134(1):9–21.
47. Murray MM, Brunet D, Michel CM (2008) Topographic ERP analyses: A step-by-step tutorial review. *Brain Topogr* 20(4):249–264.
48. Tibshirani R, Walther G (2005) Cluster validation by prediction strength. *J Comput Graph Statist* 14(3):511–528.
49. Brandeis D, Lehmann D, Michel CM, Mingrone W (1995) Mapping event-related brain potential microstates to sentence endings. *Brain Topogr* 8(2):145–159.
50. Brunet D, Murray MM, Michel CM (2011) Spatiotemporal analysis of multichannel EEG: CARTOOL. *Comput Intell Neurosci* 2011:813870.
51. Rossi S, Hallett M, Rossini PM, Pascual-Leone A; Safety of TMS Consensus Group (2009) Safety, ethical considerations, and application guidelines for the use of transcranial magnetic stimulation in clinical practice and research. *Clin Neurophysiol* 120(12): 2008–2039.